Energetic Constraints on the Creation of Cell Membrane Pores by Magnetic Particles

Timothy E. Vaughan and James C. Weaver*
Harvard-M.I.T. Division of Health Sciences and Technology, Massachusetts Institute of Technology, Cambridge, Massachusetts 02139 USA

ABSTRACT Naturally occurring and contaminant ferromagnetic and ferrimagnetic particles have been found within or near cells, and might allow pulsed magnetic fields to create transient cell membrane openings ("pores"). We show that this possibility is significantly constrained by the maximum rotational energy that can be transferred to the cell membrane. For single biologically synthesized magnetosomes (radius $r_{mag} \approx 10^{-7}$ m, magnetic moment $\mu \approx 2 \times 10^{-15}$ A m^2) and typical cell membranes, the estimated pulse magnitude must exceed $B_0 \approx 6 \times 10^{-3}$ to 7×10^{-2} T, and the optimal pulse durations are in the range 10^{-5} s $< t_{pulse} < 10^{-1}$ s. For larger contaminant particles with larger net magnetic moments, the pulse magnitudes could be only somewhat smaller, and the optimal durations are about the same. Very large pulses that exceed the coercive force of a particle are predicted to have a smaller effective magnitude and shorter effective duration.

INTRODUCTION

Magnetic particles of biological and foreign origin exist in many biological systems, including human tissues (Cohen, 1973; Gould et al., 1978; Walcott et al., 1979; Valberg, 1984; Frankel and Liburdy, 1986; Kirschvink et al., 1992a; Dunn et al., 1995). Unlike most cellular constituents, which are weakly paramagnetic or weakly diamagnetic, some of these particles have a residual magnetization in the absence of an applied magnetic field (Valberg and Butler, 1987; Kirschvink et al., 1992b). Moreover, these magnetic particles have a range of sizes and magnetic moments and have proved valuable as biophysical probes of the cytosol (Valberg and Butler, 1987). Contaminant magnetic particles are ingested or inhaled, and can have a wide range of sizes and magnetic moments. The "representative particle" treated by Valberg and Butler can be regarded as a ferromagnetic prolate ellipsoid with major axis length $a = 0.9$ μm, minor axis length $b = 0.3$ μm, and magnetic moment $\mu = 1.5 \times 10^{-14}$ A m^2. Similarly, naturally occurring, biologically synthesized magnetic particles (biogenic magnetite) have been found in many different organisms (Kobayashi and Kirschvink, 1995; Frankel and Liburdy, 1996). These naturally occurring particles exist in the form of magnetosomes, which are microscopic, bilayer membrane-encased permanent magnets. Magnetosomes possess single magnetic domains and have been found singly and in linear chains. An individual magnetosome can be regarded approximately as a sphere with radius $r_{mag} = 10^{-7}$ m and magnetic moment $\mu = 2 \times 10^{-15}$ A m^2. Magnetotactic bacteria and some animals have chains of 10 to 20 magnetosomes that are believed to be involved in magnetic sensory function. However, magnetite exists not only in magnetotactic microorganisms and some animals (Delong et al., 1993; Kobayashi and Kirschvink, 1995; Frankel and Liburdy, 1996), but also in mammalian tissues, including human brain (Kirschvink et al., 1992a,b; Dunn et al., 1995). It is generally believed that magnetotactic microorganisms use chains of magnetosomes for orientation (Kirschvink and Kirschvink, 1991), but the existence of magnetite in mammalian tissue is puzzling. Although it has been suggested that magnetic steering of chemical reactions by magnetosome membrane enzymes might occur (Kirschvink, 1994), or that magnetite might be involved in evoked epileptiform activity (Fuller et al., 1995), magnetite has no established biological function in humans. The widespread presence of both contaminant and naturally occurring magnetic particles makes them candidates for participation in biophysical mechanisms that allow magnetic fields to alter biochemical processes at the cellular level. In spite of several decades of interest in both types of particles, it is perhaps surprising that (to our knowledge) no theoretical treatment of particle-field interactions related to possible pore creation has been reported.

Accordingly, we hypothesize that interruption of the barrier function of the cell membrane might occur if pores were formed by interaction of magnetic particles with the cell membrane, because pores could lead to altered molecular transport into and out of cells, and thereby alter cellular function (Weaver, 1995; Weaver and Astumian, 1995). Without perforation by protein channels or transient pores, or involvement of shuttling carriers, the cell membrane is an imposing and extremely effective barrier against the transport of ions and charged molecules (Parsegian, 1969). In the case of temporary pores, the detailed process by which pores form in the phospholipid bilayer portion of a cell membrane is not understood in detail, even though they are believed to dominate the response of an artificial planar bilayer membrane or cell membrane to highly elevated transmembrane voltages (0.5 to 1 V). For example, electroporation is believed to involve formation of pores by a rapid

Received for publication 23 January 1996 and in final form 11 May 1996.
Address reprint requests to Dr. James C. Weaver, MIT, Harvard-MIT Division of Health Sciences and Technology, Cambridge, MA 02139. Tel.: 617-253-4194; Fax: 617-253-2514.

0006-3495/96/08/616/07 $2.00

transition from spontaneously occurring hydrophobic pores to hydrophilic pores (Abidor et al., 1979; Weaver and Chizmadzhev, 1996a,b), but the "transition states" that exist during this membrane structural rearrangement are not known. Nevertheless, considerable progress has been made in understanding electroporation by considering the energetics involved in pore formation and a statistical process of homogeneous nucleation in a bilayer membrane (Abidor et al., 1979; Weaver and Mintzer, 1981; Tsong, 1991; Weaver and Chizmadzhev, 1996a,b). Here we treat only the energetics of a hypothetical process that might result in the formation of hydrophilic pores by energy transfer from magnetic particles interacting with a magnetic field pulse. The location and mode of attachment (if any) of magnetic particles to cell membranes is not known, which provides an additional rationale for pursuing estimates based solely on energetics. Our approach therefore derives constraints that give necessary conditions for pore formation, but not sufficient conditions or the actual probability of pore occurrence.

METHODS

Our overall approach is based on the energetics governing the formation of hydrophilic pores in lipid bilayer membranes. The basic features of the magnetic field interaction of small magnetic particles within cells have been presented by others (Valberg and Butler, 1987). Translational motion is negligible because the product of a particle's magnetic moment, and the spatial field gradient, $\mu\ \partial B/\partial x$, is small for most magnetic field pulse sources. We therefore consider only the time-dependent rotational motion of a magnetic particle. The particle is characterized by its mass m_μ, moment of inertia I_μ, and magnetic moment $\vec{\mu}$; it rotates within a viscous liquid (the cytosol) and interacts with biological material represented by a torsional spring constant, κ. The corresponding one-dimensional equation of motion is

$$0 = I_\mu \ddot{\theta} + \beta_{rot}\dot{\theta} + \tau(\theta) + \kappa\theta. \quad (1)$$

Here $\tau(\theta) = \mu B(t)\sin(\theta - \theta_0)$ is the torque on the magnetosome due to the magnetic field, where θ_0 is the angle between the direction of the field pulse and the equilibrium position of the torsional spring. $\beta_{rot} = FV\eta$ is the coefficient of rotational dissipation (Berg, 1983), where F (dimensionless) is the particle's shape factor, V is its volume, and $\eta \approx 0.1$ N s m^{-2} is the viscosity of the cytosol (Valberg and Butler, 1987; Kirschvink, 1992; Adair, 1993; Polk, 1994). In addition to the single magnetosome and the representative contaminant particle, we consider a chain of 10 magnetosomes, modeled as an ellipsoid with major axis length $a = 2$ μm and minor axis length $b = 0.2$ μm, with magnetic moment $\mu = 2 \times 10^{-14}$ A m^2 (Kirschvink et al., 1992a,b; Kirschvink, 1994). Table 1 gives the values of F, V, and μ for these three representative particles.

To account for an elastic restoring force, we estimate a value for κ, a torsional spring constant, by considering stretching of the cell membrane. Little is known about how magnetic particles might be attached to cell membranes, so only an estimate is possible. An extreme case is that there is no attachment, with the magnetic particle rotating subject only to a viscous drag within the cytosol. In this case there is no energy transfer to the cell membrane and no pore creation is possible. We will not consider this case further.

A more interesting case treats the magnetic particle as a dense, rigid body that is strongly coupled to a cell membrane. In the case of a magnetosome, which is surrounded by a tightly fitting bilayer membrane with membrane proteins, localized attachment could occur by covalent bonds between adjacent pairs of membrane proteins. The energy transferred to the cell membrane need involve only a small attachment area. In the case of magnetosomes, this could involve covalent attachment between only two adjacent membrane proteins, because the bonds would be strong enough to withstand the magnetosome's motion (several hundred kT of energy are required to break a few covalent bonds). In the case of contaminant particles, for which far less is known, the case of tight attachment will provide a lower-bound constraint for the magnitude of the magnetic field pulse required for pore creation.

We make an order of magnitude estimate of κ by considering a restoring torque that accounts for the nondissipative component of cell membrane stretching. Characteristic pulse times less than about 0.1 s are needed to avoid dissipative membrane accommodation that would prevent net membrane deformation (Hochmuth and Waugh, 1987). Moreover, we assume that the elastic restoring force is associated with a strip of cell membrane with linear dimensions about the same as those of the magnetic particle, and an area elastic modulus. Therefore, we set $\kappa = A_0 K_E$, where A_0 is a characteristic area for the particle, and $K_e \approx 0.4$ N m^{-1} is the cell membrane elastic modulus (Hochmuth and Waugh, 1987). We consider two different order of magnitude estimates for A_0: 1) the product of the semimajor and semiminor ellipsoid axis lengths, and 2) the surface area of the particle. These do not provide strict limits for the participating area, but instead give an order of magnitude for plausible values (Tables 2 and 3).

To consider the energetic constraints on possible pore formation, we note that the pore creation energy is much larger than kT. In spite of the many artist's drawings in the literature, the actual structure of a hydrophilic pore is unknown (Weaver, 1993). Nevertheless, reasonable quantitative descriptions of a related phenomenon, viz. electroporation (Abidor et al., 1979; Weaver and Mintzer, 1981; Freeman et al., 1994; Weaver and Chizmadzhev, 1996a,b), have been achieved by using a cylindrical pore of radius r_p and length equal to the membrane thickness, $h \approx 7$ nm. The energy of a pore in a membrane with transmembrane voltage U is

$$W_p(r_p, U) = 2\pi\gamma r_p - \pi\Gamma r_p^2 - \frac{\pi(K_w - K_l)\varepsilon_0 U^2}{h}\int_{r_{p,min}}^{r_p} \alpha^2 r\, dr, \quad (2)$$

where γ is the edge energy density, typically $\gamma \approx 1 - 3 \times 10^{-11}$ J m^{-1}; Γ is the membrane surface tension, typically $\Gamma \approx 10^{-3}$ J m^{-2}; K_w and K_l

TABLE 1 Volumes, shape factors, and magnetic moments of magnetic particles (for the representative particles used in the simulations)

Particle	Volume [m^3]	F	μ [A m^2]
Sphere (radius = 0.1 μm)	4.2×10^{-21}	6	2.0×10^{-15}
Ellipsoid (major axis = 0.9 μm; minor axis = 0.3 μm)	4.2×10^{-20}	~16	1.5×10^{-14}
Chain (length = 2 μm)	4.2×10^{-20}	~96	2.0×10^{-14}

$\beta_{rot} = FV\eta$ is the coefficient of rotational dissipation.

TABLE 2 Area factors (product of axes) and κ values for the representative magnetic particles

Particle	A_0 [m^2]	κ [N m]
Sphere	10^{-14}	4.0×10^{-15}
Chain	10^{-13}	4.0×10^{-14}
Ellipsoid	6.8×10^{-14}	2.7×10^{-14}

$\kappa = A_0 K_E$ is the coefficient of the elastic restoring torque of the membrane, where $K_E \approx 0.4$ N m^{-1} is the area elastic modulus of the membrane material. A_0 is chosen to be the product of the semimajor and semiminor axis lengths of an ellipsoidal magnetic particle. See Table 3 footnote.

TABLE 3 Area factors (surface area) and κ values for the representative magnetic particles

Particle	A_0 [m^2]	κ [N m]
Sphere	1.3×10^{-13}	5.0×10^{-14}
Chain	9.9×10^{-13}	4.0×10^{-13}
Ellipsoid	7.0×10^{-13}	2.8×10^{-13}

A_0 is taken as the surface area of the magnetic particle. See Table 2 footnote. As discussed in the text, together Tables 2 and 3 provide order of magnitude estimates.

are the dielectric constants of water and lipid, respectively; and ε_0 is the permittivity of free space. The function α is

$$\alpha(r) = \left[1 + \frac{\pi r \sigma_p(r)}{2h\sigma_e}\right]^{-1} \quad (3)$$

and accounts for the electrical spreading resistance at the entrance and exit of the pore, hindered transport within the pore, and the Born energy repulsion that reduces the ion concentration within a pore (thereby reducing σ_p, the reduced conductivity within a pore). Here σ_e is the bulk solution conductivity, and $\sigma_p(r)$ was computed numerically by solving Poisson's equation for a series of different ion/pore configurations (Wang, 1992). This yielded a numerical solution for the electrostatic energy change, $\Delta W_{ion}(r)$, as an ion moves into a pore. The maximum value, $\Delta W_{ion,max}(r)$, is experienced at the membrane midplane and was used in a Boltzmann factor to provide a scaling factor that estimates the smaller electrical conductivity of the solution inside a pore. This results in numerical values for $\sigma_p(r)$ that are smallest for the minimum size pore, and that asymptotically approach σ_e as $r \rightarrow \infty$ (Wang, 1992).

A minimum size hydrophilic pore has $r_{p,min} \approx 1$ nm (Weaver and Chizmadzhev, 1996a,b), but for significant molecular transport somewhat larger pores should also be considered. We assume that pores with radius $r_{p,min}$ or larger must be created in the presence of a typical resting transmembrane voltage, $U \approx 0.1$ V. For values of U less than about 0.2 V and representative values of γ, Eq. 2 is well approximated by the first term. In this sense, W_p is dominated by the "edge energy" contribution. We choose the representative value $\gamma = 2 \times 10^{-11}$ J m^{-1}, which is consistent with our previous electroporation theoretical work. For $r_{p,min} = 1$ nm, the corresponding pore creation energy is

$$W_p(r_{p,min}, U = 0.1 \text{ V}) \approx 2\pi\gamma r_{p,min} \approx 30\, kT. \quad (4)$$

The appropriate values of γ are those for small pores. Electroporation experiments with artificial planar bilayer membranes have yielded inferred values of $\gamma = 3.3 \times 10^{-12}$ J m^{-1} (phosphatidylcholine), $\gamma = 8.6 \times 10^{-12}$ J m^{-1} (phosphatidylcholine in the presence of lysophosphatidylcholine), and $\gamma = 1.7 \times 10^{-11}$ J m^{-1} (phosphatidylethanolamine) along with an average pore radius $\bar{r}_p = 0.65$ nm (Chernomordik and Chizmadzhev, 1989). More direct determinations have been made for large pores using very large liposomes attached to a micropipette, and these give $\gamma = 9.2 \pm 0.7 \times 10^{-12}$ J m^{-1}, for a stearoyloleoylphosphatidylcholine membrane and $\gamma = 3.1 \pm 0.1 \times 10^{-11}$ J m^{-1} for the same membrane with 50 mol% cholesterol added (Zhelev and Needham, 1993). Thus, the literature values support the use of $\gamma = 1^{+2}_{-0.7} \times 10^{-11}$ J m^{-1}. The numerical value of γ varies with membrane composition, which could increase or decrease W_p for different cell types.

Our estimates also neglect the barrier associated with the temporary membrane structural rearrangements ("transition states") that are passed through as a pore is created. In principle these temporary rearrangements depend on how energy is coupled into the membrane, and therefore may be different from the temporary rearrangements involved in pore creation during electroporation. Moreover, although a pore's transport properties can be described by considering a small cylindrical hole in a membrane, it should be noted that pore creation involves rearrangement of membrane molecules within a region much larger than the pore's aqueous interior (Fig. 1). The temporary structural rearrangements associated with pore

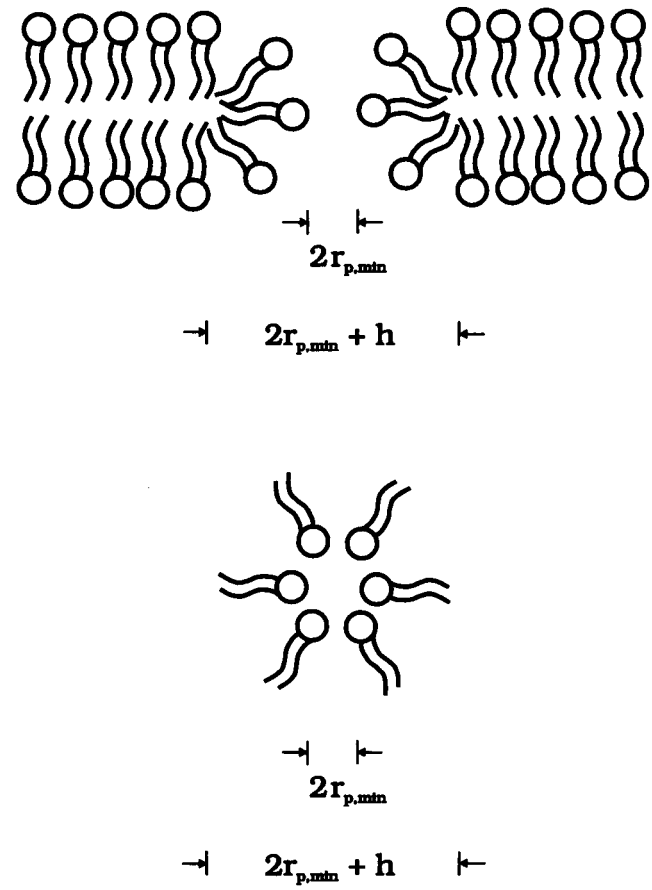

FIGURE 1 Typical drawing of a hypothetical hydrophilic pore (Abidor et al., 1979; Weaver, 1993). (*A*) Cross-sectional view along the minimum diameter, $2r_{p,min}$, of the pore opening. (*B*) Midplane view, indicating the minimum membrane area. Although the structure is not known, the depicted membrane structural rearrangement emphasizes the view that pore formation involves membrane area that significantly exceeds the pore opening, $\pi r^2_{p,min}$. The membrane thickness is $h \approx 7$ nm. As indicated by this drawing, the area of participating membrane is at least $\pi(r_{p,min} + h/2)^2$.

formation may involve a still larger membrane area than those involved in the "final state" that includes a pore. As illustrated in Fig. 1, this minimum area of membrane involvement in the final, pore-containing state is

$$A_{m,min} \approx \pi\left[r_{p,min} + \frac{h}{2}\right]^2, \quad (5)$$

where h is the membrane thickness. Inspection of Fig. 1 shows that a circular patch of membrane with minimum diameter $2r_{p,min} + h$ must be involved in the temporary structural rearrangement associated with pore formation. Thus, the membrane area involved in pore creation is much larger than $\pi r^2_{p,min}$, and elastic energy deposited in the membrane over the larger area may be able to contribute to pore formation.

Our approach to estimating an energetic bound for pore creation assumes that the maximum elastic energy transiently stored in the membrane originates from the rotating magnetic particle. This maximum possible energy transfer is equal to the rotational elastic work

$$W_{rot,elas} = \int_0^{(\Delta t)_{pulse}} \kappa\theta\dot{\theta}\, dt, \quad (6)$$

and was computed using numerical solutions to Eq. 1. To provide insight into what is important, we used three different magnetic pulse shapes to estimate values of B_0 needed to create a pore: 1) a half period sine wave, $B(t) = B_0 \sin(\pi t/(\Delta t)_{pulse})$; 2) a ramp, $B(t) = B_0 t/(\Delta t)_{pulse}$ (the rising portion of the pulse); and 3) an exponentially decaying pulse, $B(t) = B_0 \exp(-t/(\Delta t)_{pulse})$. In each case $(\Delta t)_{pulse}$ is a characteristic time of the magnetic field pulse. For the half period sine wave, $(\Delta t)_{pulse}$ is one-half the period, so the frequency of the pulse is $f = 1/(2(\Delta t)_{pulse})$.

A numerical solution has the advantage that quantitative results can be obtained for a wide range of conditions, but the disadvantage is that the dependence on basic parameters is not apparent. However, in the limit of long-duration pulses and negligible viscous dissipation we can obtain an analytic expression that is independent of pulse shape details, because pulses of equal magnitude, B_0, result in equal energy deposition into the membrane. As shown in the Appendix, in this limit the energy is

$$W_{rot,elas} \approx \frac{\mu^2 B_0^2}{2\kappa}. \tag{7}$$

Equation 7 leads immediately to the peak field magnitude needed for possible pore creation,

$$B_0 \approx \frac{\sqrt{2\kappa W_{rot,elas}}}{\mu} \approx \frac{\sqrt{4\pi\gamma r_{p,min} A_0 K_E}}{\mu}. \tag{8}$$

Equation 8 shows the dependence of B_0 on basic parameters of the model. In particular, we note that for a chain of N_{chain} magnetosomes, both the area factor, A_0, and the magnetic moment, μ, are proportional to N_{chain}, so B_0 varies as $N_{chain}^{-1/2}$. In the case of chains of different size magnetosomes, μ can be scaled appropriately to estimate the peak field.

It is useful to distinguish "long-duration" pulses, i.e., those with characteristic times longer than $(\Delta t)_{pulse} \approx \beta/\kappa$. For pulses that are shorter than β/κ, significant energy is dissipated within the cytosol, and B_0 must exceed these values to create a pore. For the range of κ used here, $\beta/\kappa \approx 10^{-6}$ s to 10^{-5} s, so $(\Delta t)_{pulse}$ must be longer than this for most of the magnetic work to go into the potential energy of the effective torsional spring, with almost none dissipated by the frictional force. Such pulses are therefore the most "efficient" for possible pore creation.

It should be noted that the response of magnetic particles to magnetic field pulses is predicted to be extremely rapid. For example, consider a single magnetosome in the purely viscous case (zero restoring torque), for which the characteristic time to reach terminal rotational velocity is $\tau_{rot} = I_\mu/\beta \approx 10^{-10}$ s. This extremely short relaxation time indicates that inertial effects are not important for the time scales that we have considered.

A final consideration is the possibility that the pulse exceeds the coercive force, H_c, of the magnetosome. If $B_0 > \mu_0 H_c$, then the magnetization itself can shift to a new orientation with respect to the particle. That is, the direction of $\vec{\mu}$ is altered, but the particle itself does not rotate further. For a spherical particle the coercive force is determined by the magnetocrystalline anisotropy, and is given by

$$H_c = \frac{2K_1}{\mu_0 J_s}, \tag{9}$$

where K_1 is the anisotropy energy density constant, J_s is the magnetization, and μ_0 is the permeability of free space (Kittel, 1949). $\mu_0 = 4\pi \times 10^{-7}$ N A^{-2}, and for magnetite, $K_1 = 1.3 \times 10^4$ J m^{-3} and $J_s = 4.8 \times 10^5$ A m^{-1}. The field strength that can reorient the magnetic moment without additional particle rotation is therefore

$$B_c = \mu_0 H_c = \frac{2K_1}{J_s} = 5.4 \times 10^{-2}\ \text{T} \tag{10}$$

for a spherical particle.

For each sphere in a chain, the coercive force will be somewhat larger than that of an isolated sphere, because the other spheres in the chain help enforce the magnetization direction. For simplicity, however, we also use Eq. 10 for a chain, recognizing that it provides a lower limit for B_c. For the ellipsoidal particle representing a contaminant particle, Valberg and Butler (1987) report the coercive field strength $B_c = 2.5 \times 10^{-2}$ T, and we use this value.

The concept of an "effective pulse" can be used to estimate energetic constraints for very large magnetic field pulses that exceed B_c. Specifically, the time at which a pulse reaches a magnitude of B_c defines an effective pulse duration, $(\Delta t)_{pulse,eff}$, because only this initial portion of the pulse can rotate the magnetic particle. In the case of a very large pulse with a nearly linear rise, this gives the relation

$$(\Delta t)_{pulse,eff} \approx \left[\frac{B_c}{B_0}\right](\Delta t)_{pulse}; \quad B_0 > B_c. \tag{11}$$

This effective pulse length is dependent on the nature of the magnetic particle, because B_c depends on both composition and particle geometry. Very large magnetic field pulses that have a leading edge that can be approximated by a ramp are therefore expected to have energetic constraints in which $(\Delta t)_{pulse,eff}$ replaces the complete pulse rise time. Moreover, the effective pulse magnitude is reduced to

$$B_{0,eff} = B_c, \tag{12}$$

so that the two effective values of Eqs. 11 and 12 greatly constrain the ability of very large pulses to satisfy the energetic constraints for membrane pore creation.

RESULTS AND DISCUSSION

Figs. 2–4 each show results of numerical simulations that use Eq. 1 to determine the smallest magnetic field magnitude that achieves 30 kT for the elastic energy term. This energy could therefore be available to the membrane for

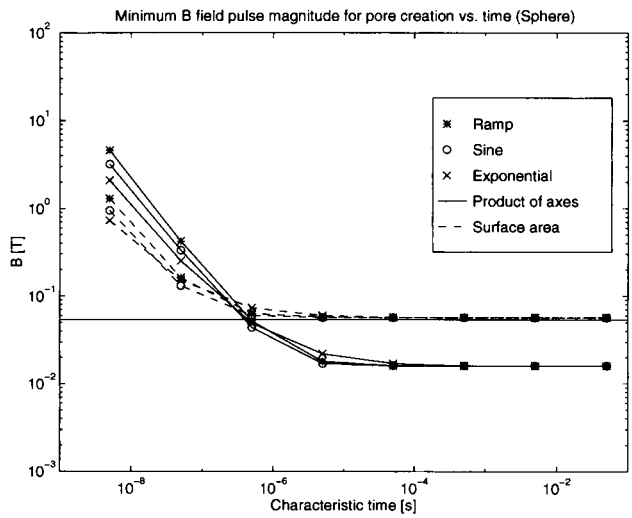

FIGURE 2 Theoretical predictions of the minimum magnetic field pulse magnitude, B_0, for pore creation plotted against the pulse duration, $(\Delta t)_{pulse}$, for a single magnetosome. Two families of curves are plotted, corresponding to the two choices of area factor (see text and Tables 1–3). The predicted values of B_0 are plotted for three different pulse shapes: a ramp, a half sine wave, and an exponential (see text). The fact that similar behavior was obtained for three different, idealized pulses supports the conclusion that the pulse shape is relatively unimportant, and that the peak magnetic field is the most important attribute of the pulse. The horizontal line labeled B_c indicates the coercive force for a single magnetosome. Above B_c the magnetic moment can reorient with respect to the magnetosome, such that the magnetosome does not rotate further.

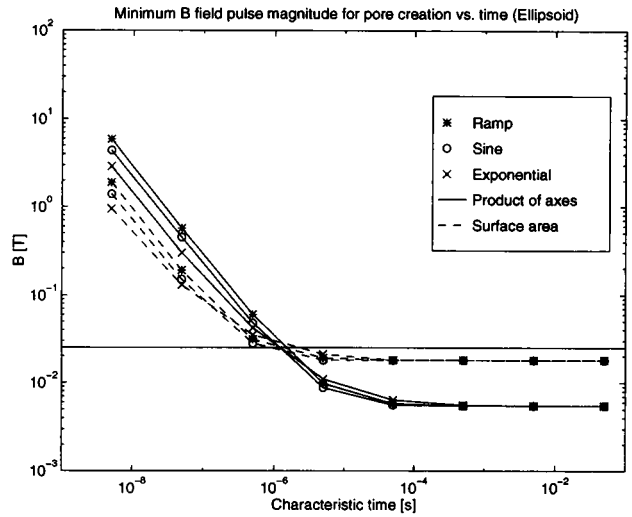

FIGURE 3 Same as Fig. 2, but for an ellipsoidal particle that represents a typical magnetic contaminant.

possible pore creation. All of these numerical results show that a huge magnetic field magnitude is needed for short pulse durations, viz. $(\Delta t)_{\text{pulse}} < 10^{-6}$ to 10^{-5} s. The transition region between "short" and "long" pulses is not exactly the same for all of the computed cases, because the value of β/κ is different in each case. As shown in Fig. 2, for the spherical magnetic particle the transition region is around 10^{-6} s to 10^{-5} s for the "product of axes" area ($A_0 = 10^{-14}$ m^2), but is displaced by about an order of magnitude toward shorter times of about 10^{-7} s to 10^{-6} s for the "surface area" case ($A_0 = 1.3 \times 10^{-13}$ m^2), which has a 13-fold larger area. A larger effective area results in a larger viscous drag, so even for relatively longer duration pulses with their smaller angular velocities, the viscous effects become important. The smaller area case, however, leads to a smaller predicted field magnitude, about $B_0 = 1.6 \times 10^{-2}$ T compared to 5.7×10^{-2} T for the "surface area" case. This dependence on the area is evident from Eq. 8.

Similar behavior is shown in Fig. 3, for the ellipsoidal particle, which represents a typical magnetic contaminant. This larger particle has a much larger magnetic moment ($\mu_{\text{ellip}} \approx 1.5 \times 10^{-14}$ A m^2, compared with $\mu_{\text{sphere}} \approx 2 \times 10^{-15}$ A m^2), but also has a bigger area factor. The resulting greater value of κ leads to a transition region at a longer pulse duration, as expected. However, the greater magnetic moment gives a smaller predicted field value for the long-duration pulses: $B_0 = 5.5 \times 10^{-3}$ T for the "product of axes" case, and 1.8×10^{-3} T for the "surface area" case.

Fig. 4 shows that the predicted results for a chain of 10 magnetosomes are nearly the same as for the ellipsoidal particle. In this case the magnetic moment is slightly higher ($\mu_{\text{chain}} \approx 2 \times 10^{-14}$ A m^2), as are the two area factors. The predicted field magnitude for long-duration pulses is $B_0 = 5.1 \times 10^{-3}$ T for the "product of axes" case, and 1.6×10^{-3} T for the "surface area" case.

It should be noted that the analytic expression for the pulse magnitude (Eq. 8) is valid for the longer duration pulses, where the predicted pulse magnitude is the smallest. This is presumably the region of greatest interest for experimental testing of the hypothesis that magnetic particles interacting with magnetic field pulses can create membrane pores. Moreover, it is presumably most relevant to concerns relating to exposure of humans to magnetic fields. This is also the region where the dependence on the parameters of the model can be most easily seen (Eq. 8). Thus, for example, if we had used $\gamma = 3 \times 10^{-12}$ J m^{-1} rather than $\gamma = 2 \times 10^{-11}$ J m^{-1}, all of the predicted field values for B_0 would be smaller, by almost a factor of 2.6. Thus, for example, a spherical magnetosome with the smaller area factor has a predicted value $B_0 \approx 6 \times 10^{-3}$ T.

Both the analytic limiting expression and the numerical simulations support the same conclusion: the most important aspect of a magnetic field pulse is its magnitude, B_0. The predicted values of B_0 as a function of $(\Delta t)_{\text{pulse}}$ for the three pulse types show that there are significant constraints on the interaction of small magnetic particles, such as magnetosomes, with time-varying magnetic fields, and Figs. 3 and 4 show that larger magnetic particles are only somewhat less constrained. For pulses longer than about 10^{-5} s, the field magnitude threshold is expected to be approximately independent of pulse duration down to about 0.1 s. For the single magnetosome that we considered, the threshold field is $B_0 \approx 6 \times 10^{-3}$ to 7×10^{-2} T for pulse durations in the range $(\Delta t)_{\text{pulse}} = 10^{-5}$ s to 10^{-1} s. As expected, if larger magnetic moments are involved, the predicted fields are smaller. It is clear from Fig. 2 that the field magnitude threshold is independent of pulse shape for the longer pulse durations. During these long pulses, very little energy is dissipated within the cytosol, and in this case all the magnetic work could be deposited temporarily into the membrane as elastic energy, as a prelude to pore creation. There-

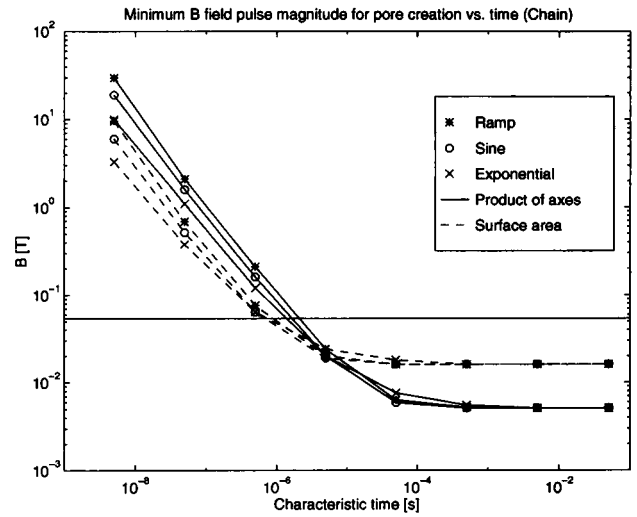

FIGURE 4 Same as Fig. 2, but for a linear (rigid) chain of $N_{\text{chain}} = 10$ magnetosomes.

fore, the potential ability to create pores depends only on the peak value of the field, B_0, not on the detailed behavior before and after this peak is reached.

Magnetic field pulses for biomagnetic stimulation of nerves by their induced electric fields are intended to initiate action potentials (Barker et al., 1985; Ueno, 1994) and are candidates for creating membrane pores by interacting with magnetic particles. A typical pulse has an approximately linear rise to 2 T within the first 100 μs, and then decays relatively slowly (Barker, 1994). The pulse rise time (10^{-4} s) is itself well within the pulse duration region for the smallest B_0 values (Figs. 2–4). However, considering the almost linear rise, for an ellipsoidal contaminant particle, the coercive force field, $B_c = 2.5 \times 10^{-2}$ T, is exceeded after about only 1×10^{-6} s. This implies that the effective pulse capable of rotating the magnetic particle has magnitude $B_{0,\text{eff}} \approx 2.5 \times 10^{-2}$ T, and this effective pulse has a much shorter effective duration, $(\Delta t)_{\text{pulse,eff}} \approx 1 \times 10^{-6}$ s. Inspection of Fig. 2 shows that the effective pulse lies within the region where viscous dissipation begins to become important. Specifically, for $(\Delta t)_{\text{pulse,eff}} \approx 1 \times 10^{-6}$ s, a pulse of magnitude $B_0 \approx B_c$ is required (Fig. 3). Thus, perhaps surprisingly, this type of biomagnetic stimulation pulse interacting with a typical contaminant magnetic particle barely satisfies the energetic constraints for creating a pore. However, in the case of a spherical magnetosome ($B_c = 5.4 \times 10^{-2}$ T), the effective pulse duration is $(\Delta t)_{\text{pulse,eff}} \approx 2 \times 10^{-6}$ s. Inspection of Fig. 1 shows that for this effective pulse duration the required field magnitude is smaller, $B_0 \approx 2 \times 10^{-2}$ T $< B_c$. Thus, pore creation involving individual magnetosomes may be possible. Were this to occur, chemical exchange between the intra- and extracellular compartments could be increased. Given the finding of biological magnetite in human brain tissue, this possible interaction should be considered along with the intended induced electric field nerve stimulation. Interestingly, the magnetically induced electric field is extremely large, ranging from about 100 to 500 V m^{-1} over the first 100 μs of the pulse (Barker, 1994). Electric fields widely used to cause electroporation of mammalian cells are about two orders of magnitude larger in magnitude, and usually of about one order of magnitude longer duration (Weaver and Chizmadzhev, 1996a,b). The observation that low-frequency (0.1 to 1 Hz) fields of order 5×10^3 to 2×10^4 V m^{-1} can cause cellular uptake of DNA (Xie and Tsong, 1990) suggests that multiple pulses of the magnitude used in magnetic stimulation could be investigated, but is beyond the scope of this paper. Similarly, the rare but large magnetic field pulse associated with quenching of superconducting magnets such as those used in magnetic resonance imaging could be considered.

We emphasize that this analysis does not predict that pores are created, only that energetics impose significant constraints. However, the hypothesis that pores can be created by an interaction between magnetic field pulses and magnetic particles near cells could be tested experimentally using methods developed for electroporation studies. Charged, normally impermeant fluorescent molecules could be provided extracellularly; then, different magnetic pulsing conditions can be tested to see which ones cause a subpopulation of cells to take up these otherwise impermeant molecules (Prausnitz et al., 1994; Gift and Weaver, 1995). The theoretical estimates presented in this paper provide strong energetic constraints on what types of pulses could lead to molecular uptake by a hydrophilic pore creation mechanism.

APPENDIX

For magnetic pulses of long enough duration [$(\Delta t)_{\text{pulse}} \gg \beta/\kappa$], negligible energy will be associated with the viscous term of Eq. 1. Instead, essentially all of the energy of the magnetic field pulse will be represented by the elastic term. The interaction energy can be most easily calculated by considering the torques involved. If there is negligible dissipation by the viscous liquid, the torsional spring is quasistatically stretched by the twisting magnetic particle, such that the elastic restoring torque matches the applied magnetic torque at all times,

$$\kappa\theta(t) = \mu B(t). \tag{A1}$$

Note that we have used the linearized equation, which is valid if the pulse magnitude is not too large compared to κ/μ. Therefore, the maximum rotation angle of the magnetic particle occurs at the peak field value,

$$\theta_{\max} = \frac{\mu B_0}{\kappa}, \tag{A2}$$

and the maximum rotational elastic energy is

$$W_{\text{rot,elas}} = \frac{1}{2}\kappa\theta_{\max}^2 = \frac{\mu^2 B_0^2}{2\kappa}, \tag{A3}$$

which is Eq. 7. Note that this equation is independent of the pulse shape.

We thank M. Vance, J. L. Kirschvink, E. A. Gift, Y. Chizmadzhev, and R. K. Adair for stimulating and critical discussions.

This work supported partially by NIH Grant ES06010 in the early phases, DOE Contract No. 19X-ST613C in the final phases, and a computer equipment grant from Stadwerke Düsseldorf, Düsseldorf, Germany.

REFERENCES

Abidor, I. G., V. B. Arakelyan, L. V. Chernomordik, Yu. A. Chizmadzhev, V. F. Pastushenko, and M. R. Tarasevich. 1979. Electric breakdown of bilayer membranes. I. The main experimental facts and their qualitative discussion. *Bioelectrochem. Bioenerget.* 6:37–52.

Adair, R. K. 1993. Effects of ELF magnetic fields on biological magnetite. *Bioelectromagnetics.* 14:1–4.

Barker, A. T. 1994. Magnetic nerve stimulation: principles, advantages and disadvantages. *In* Biomagnetic Simulation. S. Ueno, editor, Plenum Press, New York. 9–28.

Barker, A. T., R. Jalinous, and I. L. Freeston. 1985. Non-invasive stimulation of the human motor cortex. *Lancet.* i:1106–1107.

Berg, H. C. 1983. Random Walks in Biology. Princeton University Press, Princeton, NJ.

Chernomordik, L. V., and Y. A. Chizmadzhev. 1989. Electrical breakdown of lipid bilayer membranes: phenomenology and mechanism. *In* Electroporation and Electrofusion in Cell Biology. E. Neumann, A. E. Sowers, and C. A. Jordan, editors. Plenum, New York. 83–95.

Cohen, D. 1973. Ferromagnetic contaminants in the lungs and other organs of the body. *Science.* 180:745–748.

DeLong, E. F., R. B. Frankel, and D. A. Bazylinski. 1993. Multiple evolutionary origins of magnetotaxis in bacteria. *Science.* 259:803–806.

Dunn, J. R., M. Fuller, J. Zoeger, J. Dobson, F. Heller, J. Hammann, E. Caine, and B. M. Moskowitz. 1995. Magnetic material in the human hippocampus. *Brain Res. Bull.* 36:149–153.

Frankel, R. B., and R. P. Liburdy. 1996. Biological effects of static magnetic fields. *In* CRC Handbook of Biological Effects of Electromagnetic Fields, 2nd Ed. C. Polk and E. Postow, editors. CRC Press, Boca Raton. 149–183.

Freeman, S. A., M. A. Wang, and J. C. Weaver. 1994. Theory of electroporation for a planar bilayer membrane: predictions of the fractional aqueous area, change in capacitance and pore-pore separation. *Biophys. J.* 67:42–56.

Fuller, M., J. Dobson, H. G. Wieser, and S. Moser. 1995. On the sensitivity of the human brain to magnetic fields: evocation of epileptiform activity. *Brain Res. Bull.* 36:155–159.

Gift, E. A., and J. C. Weaver. 1995. Observation of extremely heterogeneous electroporative uptake which changes with electric field pulse amplitude in *Saccharomyces cerevisiae. Biochim. Biophys. Acta.* 1234: 52–62.

Gould, J. L., J. L. Kirschvink, and K. S. Deffeyes. 1978. Bees have magnetic remanence. *Science.* 201:1026–1028.

Hochmuth, R. M., and R. E. Waugh. 1987. Erythrocyte membrane elasticity and viscosity. *Am. Rev. Physiol.* 49:209–219.

Kirschvink, J. L. 1992. Constraints on biological effects of weak extremely low frequency electromagnetic fields: comment. *Phys. Rev. A.* 46: 2178–2184.

Kirschvink, J. L. 1994. Rock magnetism linked to human brain magnetite. *Trans. Am. Geophys. Union.* 75:178–179.

Kirschvink, J. L., and A. K. Kirschvink. 1991. Is geomagnetic sensitivity real? Replication of the Walker-Bitterman magnetic conditioning experiment in honey bees. *J. Am. Zool.* 31:169–185.

Kirschvink, J. L., A. K. Kirschvink, and B. J. Woodford. 1992a. Magnetite biomineralization in the human brain. *Proc. Natl. Acad. Sci. USA.* 89:7683–7687.

Kirschvink, J. L., A. Kobayashi-Kirschvink, J. C. Diaz-Ricci, and S. J. Kirschvink. 1992b. Ferromagnetic material in human tissue: implications for background levels of ELF exposure. *Bioelectromagnetics Suppl.* 1:101–113.

Kittel, C. 1949. Physical theory of ferromagnetic domains. *Rev. Mod. Phys.* 21:541–583.

Kobayashi, A. K., and J. L. Kirschvink. 1995. Magnetoreception and electromagnetic field effects: sensory perception of the geomagnetic field in animals and humans. *In* Electromagnetic Fields: Biological Interactions and Mechanisms. M. Blank, editor. American Chemical Society, Washington, DC. 367–394.

Parsegian, V. A. 1969. Energy of an ion crossing a low dielectric membrane: solutions to four relevant electrostatic problems. *Nature.* 221:844–846.

Polk, C. 1994. Effects of ELF fields on biological magnetite: limitations on physical models. *Bioelectromagnetics.* 15:261–270.

Prausnitz, M. R., C. D. Milano, J. A. Gimm, R. Langer, and J. C. Weaver. 1994. Quantitative study of molecular transport due to electroporation: uptake of bovine serum albumin by human red blood cell ghosts. *Biophys. J.* 66:1522–1530.

Tsong, T. Y. 1991. Electroporation of cell membranes. *Biophys. J.* 60: 297–306.

Ueno, S., editor. 1994. Biomagnetic Simulation. Plenum Press, New York.

Valberg, P. A. 1984. Magnetometry of ingested particles in pulmonary macrophages. *Science.* 224:513–516.

Valberg, P. A., and J. P. Butler. 1987. Magnetic particle motions within living cells: physical theory and techniques. *Biophys. J.* 52:537–550.

Walcott, C., J. L. Gould, and J. L. Kirschvink. 1979. Pigeons have magnets. *Science.* 205:1027–1029.

Wang, M. A. 1992. Electroporation: description of a quantitative theory and its application to molecular transport. S. B. thesis. MIT, Cambridge.

Weaver, J. C. 1993. Electroporation: a dramatic, non-thermal electric field phenomenon. *In* Electricity and Magnetism in Biology and Medicine. 95–100.

Weaver, J. C. 1995. Electroporation in cells and tissues: a biophysical phenomenon due to electromagnetic fields. *Radio Sci.* 30:205–221.

Weaver, J. C., and R. D. Astumian. 1995. Issues relating to causality of bioelectromagnetic effects. *In* Environmental Electric and Magnetic Fields. M. Blank, editor. American Chemical Society, New York. 79–96.

Weaver, J. C., and Y. A. Chizmadzhev. 1996a. Electroporation. *In* CRC Handbook of Biological Effects of Electromagnetic Fields, 2nd Ed. C. Polk and E. Postow, editors. CRC Press, Boca Raton. 247–274.

Weaver, J. C., and Y. A. Chizmadzhev. 1996b. Theory of electroporation: a review. *Bioelectrochem. Bioenerget.* In press.

Weaver, J. C., and R. A. Mintzer. 1981. Decreased bilayer stability due to transmembrane potentials. *Phys. Lett.* 86A:57–59.

Xie, T.-D., and T. Y. Tsong. 1990. Study of mechanisms of electric field-induced DNA transfection II: transfection by low amplitude, low frequency alternating electric fields. *Biophys. J.* 58:897–903.

Zhelev, D. V., and D. Needham. 1993. Tension-stabilized pores in giant vesicles: determination of pore size and pore line tension. *Biochim. Biophys. Acta.* 1147:89–104.